



Universiteit
Leiden
The Netherlands

Exploring charge transport properties and functionality of molecule-nanoparticle ensembles

Devid, E.J.

Citation

Devid, E. J. (2015, December 17). *Exploring charge transport properties and functionality of molecule-nanoparticle ensembles*. *Casimir PhD Series*. Retrieved from <https://hdl.handle.net/1887/37091>

Version: Not Applicable (or Unknown)

License: [Leiden University Non-exclusive license](#)

Downloaded from: <https://hdl.handle.net/1887/37091>

Note: To cite this publication please use the final published version (if applicable).

Cover Page



Universiteit Leiden



The handle <http://hdl.handle.net/1887/37091> holds various files of this Leiden University dissertation.

Author: Devid, Edwin Johan

Title: Exploring charge transport properties and functionality of molecule-nanoparticle ensembles

Issue Date: 2015-12-17

2

Charge transport in molecular systems

In this Chapter, a basic description of the conductance properties of molecular junctions is given. First, I briefly introduce charge transport at low length scales, leading to the concept that conductance can be described in terms of electron wave transmission. Next, the transmission function $T(E)$ of a molecular junction and its relation to the molecular orbital structure is discussed, specifically for spin transition compounds.

2.1 Charge transport on the macroscopic scale

To appreciate molecular charge transport as a quantum phenomenon, let us start on the macroscopic scale. The classical Ohm's Law states that the current I , running through a macroscopic conductor, is linearly related to the applied voltage bias V via $I = V/R$. The proportionality constant between the two is the resistance R . This simple law holds for metal wires within the classical Drude picture. Here, the charge carriers (electrons) are seen as small diffusing particles scattering off defects and phonons in an atomic lattice. This gives rise to a mean free path, l_e and a finite conductance $G = 1/R$. The question naturally arises what happens to the conductance if the conducting wire is reduced to length scales shorter than the mean free path.

2.2 Charge transport at reduced length scales

Let us next consider a junction for which the mean free path exceeds the length of the 'wire' L . Moreover, we will consider that $L < l_e, l_\phi$, where l_ϕ is the phase coherence length. In that case, the wavelike properties (phase) of the electrons become relevant and the conductance needs to be described from a quantum mechanics perspective. The 'wire' in this case could be a single gold atom (diameter $\sim 2.5 \text{ \AA}$) or a molecule (typically a few nanometers in length) contacted by two electrodes. However, it may also be a narrow constriction (quantum point contact) defined in a two-dimensional electron gas [1, 2].

If there is virtually no scattering within the wire, the conductance will only be limited by the constriction itself. Sharvin [3, 4] approximated this problem in a semi-classical way, assuming $\lambda_F \ll L \ll l_e, l_\phi$, where λ_F is the Fermi wavelength. This case is comparable to that of a diluted gas flowing through an opening of radius r under a slight pressure difference between the chambers left and right of the constriction. When the potential difference is eV , the electrons will change their velocity by $\Delta v = \pm eV/p_F$ when passing the opening. (Here $p_F = \hbar k_F = h/\lambda_F$ is the Fermi momentum, h is Planck's constant and $\hbar = h/2\pi$). Now, the net current will be $I = ne\Delta v S$, where $S = \pi r^2$ is the area of the orifice. Taking into account Fermi-Dirac statistics for the electron density n , the conductance for a circular ballistic point contact becomes:

$$G \approx \frac{2e^2}{h} \left(\frac{\pi r}{\lambda_F} \right)^2 = \frac{2e^2}{h} \left(\frac{k_F r}{2} \right)^2. \quad (2.1)$$

Note that the conductance found is independent of the length of the wire, as expected for ballistic transport. It is only determined by the electron density (via p_F) and the orifice's radius r . Interestingly, the constant $G_0 = 2e^2/h = (12.9 \text{ k}\Omega)^{-1}$ emerged in this equation. Often denoted the quantum of conductance, it will generally appear in equations describing quantum charge transport.

The Sharvin approach is semi-classical and will break down as the width of the constriction approaches the electron wavelength. To describe charge transport in a fully quantum mechanical way, we follow R. Landauer [5]. He was the first to realize that electrical conductance can be described in terms of transmission and reflection probabilities of electron waves. To appreciate this, let us again assume a constriction in a metal conductor (with length L and width W), contacted by two electrodes (see Figure 2.1(a)). The lateral confinement, will only allow for a discrete number of transverse states with energy below the Fermi level of the conduction electrons in the leads. Intuitively these eigenstates or modes can be seen as those for which a transverse standing wave is formed, i.e. they have $i\lambda/2 = W$, where i is an integer and λ is the electron wavelength. Landauer realized that each of these states gives rise to a so-called conductance channel. Incoming electrons coupling into a state i will hence be transmitted with a certain probability T_i . The maximum transmission equals 1 (no reflection), which gives rise to a conductance of exactly $G_0 = 2e^2/h$ (assuming spin degeneracy).

More generally, the conductance is obtained by summing up the transmission values connected to all N conductance channels in the scatterer, i.e.

$$G = \frac{2e^2}{h} \sum_{i=1}^N T_i, \quad (2.2)$$

where $0 \leq T_i \leq 1$ denote the transmission values of each of the N channels.

Interestingly, this formula also holds if an elastic scatterer is present in the constriction (see Figure 2.1(b)). In that case, a scattering matrix is used to connect outgoing states and ingoing states phase coherently [4, 6]. This matrix can hence be written in this form:

$$\hat{S} = \begin{pmatrix} r & t' \\ t & r' \end{pmatrix}, \quad (2.3)$$

where t and t' represent the transmission amplitudes to the right and left electrodes respectively. Similarly, r and r' represent the reflection amplitudes toward the left and

right electrodes respectively. As a result of conservation of current, $tt^\dagger + rr^\dagger = t^\dagger t^\dagger + r^\dagger r^\dagger$. Now, the eigenvalues of tt^\dagger correspond to the transmission probabilities T_i in equation 2.2.

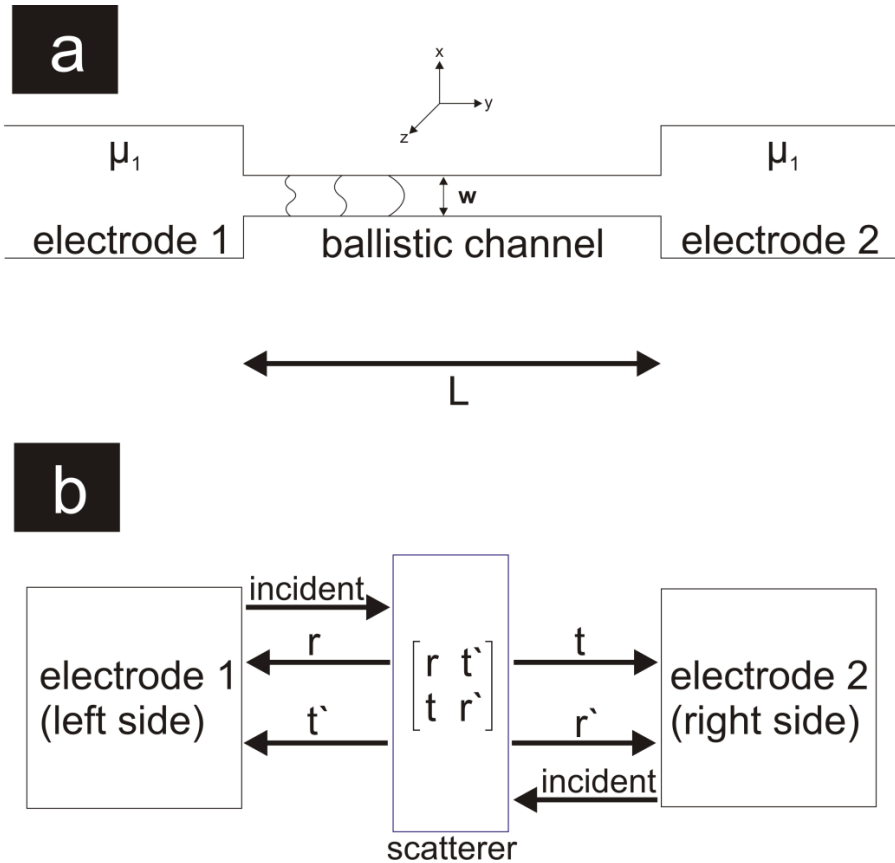


Figure 2.1: (a) Schematic representation of a ballistic channel of length L , width W and height H . The electrons travel through this narrowing channel while they are confined in the y - and z - directions. Here, only transversal wavelengths are allowed with $\lambda_x = 2W/i$ and $\lambda_z = 2H/j$ (here i, j are integers). The channel separates the two electrodes with electrochemical potentials μ_1 and μ_2 . (b) Schematic representation of the transmission formalism, where the channel is assumed to be connected to the electrodes. Here, the channel can be viewed as a quantum wire with multiple subbands. The one-channel scatterer can be defined by a S-matrix that relates the incoming and outgoing amplitudes. The presence of a scatterer in one transverse channel gives rise to transmission and reflection eigenstates.

Experimentally, conductance quantization was discovered using constrictions in two-dimensional electron gases. As the constriction was gradually closed (using negatively polarized side gates), the number of transmission channels decreased discretely and hence the conductance went down stepwise. Such experiments formed the first clear proof of the Landauer formula in equation 2.2 [1, 2, 7].

2.3 Charge transport through a molecular junction

After reviewing the charge transport properties of a nanoscopic metal conductor, let us focus on charge transport through a molecular junction. Here, two metal electrodes called the source and the drain (also called contacts or reservoirs) are connected by a molecule with a specific length L . Charge transport through such a device is dominated by the molecular energy levels, by their coupling to the reservoirs and, in some regime, by the charging energy E_C of the molecule (if coupling is weak). In general, the energy level separation for organic molecules is much larger than the thermal energy $k_B T$, even at room temperature, emphasizing the need to describe molecular charge transport as a form of quantum transport.

For a free molecule, the energy level (eigenvalues connected to the molecular orbitals) are discrete and well-defined. This can be understood within the Heisenberg uncertainty relations. Electrons have no way to hop off the molecule, i.e. the residence time τ is very high, and as a result the uncertainty in the energy of a level is very small. This changes once a molecule is coupled to electrodes. In that case, electrons can coherently move in and out of the molecule, decreasing τ and hence leading to a significant uncertainty of the energy level value. This is referred to as level broadening. Note that this is the case even with no bias present ($V_b = 0$). Level broadening plays an important role in charge transport, as we shall see below. Note that in a more chemical picture, level broadening can be understood in terms of hybridization between a molecular level and the bands in the metal electrodes.

To describe transport, we next need the electron distribution in the electrodes. It is given by the Fermi-Dirac function:

$$f_0(E - \mu) = \frac{1}{1 + e^{\frac{E - \mu}{k_B T}}}, \quad (2.4)$$

where μ denotes the electrochemical potential at an electrode. At 0 K, the states below μ are occupied, so $f_0 = 1$, whereas bands with energy above μ are empty, i.e. the

distribution is a step function. But at room temperature ($k_B T \approx 25$ meV) the distribution is smeared out around μ and $0 \leq f_0 \leq 1$ [8, 9].

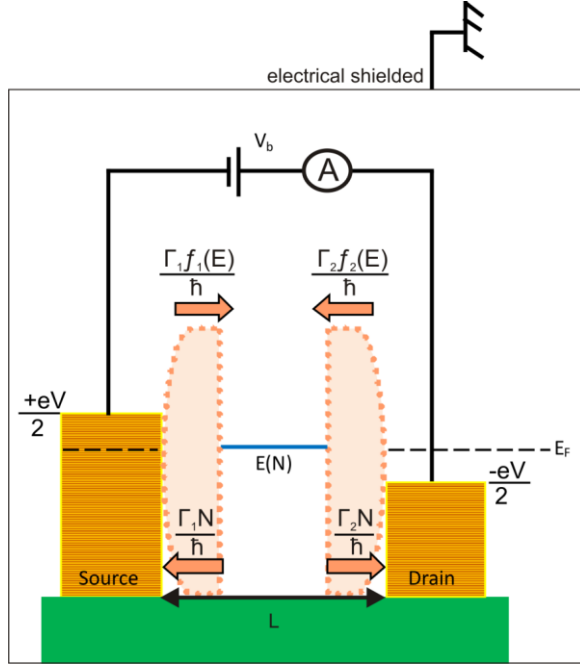


Figure 2.2: Scheme of the transfer of electrons through a molecular junction connected to the source and the drain. The molecular junction considered has a sharp energy level and symmetric coupling to the leads. The orange arrows display the net flux of electrons in and out of a one-level molecular channel.

By applying a bias V_b between the source and drain metal electrodes, the electrochemical potentials, μ_1 and μ_2 respectively, will differ by:

$$\mu_1 - \mu_2 = eV_b. \quad (2.5)$$

Now, there can be a net electron flow towards the anode. However, electrons can only flow from an occupied energy level in one electrode to an unoccupied state in the other contact, via a broadened molecular level. If coupling to the electrodes is relatively strong, electron waves will be delocalized over the junction and charge transport can be considered coherent. In the case that the metal Fermi levels line up with a molecular

level, one speaks of resonant charge transport. In that regime, transmission can be near unity. More generally, however, transport is via the tails of the broadened molecular energy levels. This is referred to as off-resonant transport. Clearly, this calls for an extension of Landauer's formula in order to include a continuous energy dependence of the transmission.

To do so, let us consider level broadening in more detail. Following Figure 2.2, we denote Γ_1/\hbar and Γ_2/\hbar as the rate constants from which an electron on energy level $E(N)$ will move in and out of the source and the drain electrodes respectively. Hence, $\Gamma_{1,2}$ has the dimension of energy. Broadening gives rise to a Lorentzian density of states (DOS) for a level at energy ε [9]

$$D_\varepsilon(E) = \frac{\Gamma/2\pi}{(E-\varepsilon)^2 + (\Gamma/2)^2}. \quad (2.6)$$

Here, $\Gamma = \Gamma_1 + \Gamma_2$, i.e. the level broadening is due to coupling to both electrodes (see Figure 2.3). Now, the current flowing through the junction is given by integrating over all possible electron energies, incorporating the DOS and the coupling factors, i.e.:

$$I = \frac{2e}{\hbar} \int_{-\infty}^{+\infty} D_\varepsilon(E) \frac{\Gamma_1\Gamma_2}{\Gamma} [f_1(E) - f_2(E)] dE. \quad (2.7)$$

This incorporates a spin degeneracy in the energy levels, giving rise to the prefactor 2. At 0 K, then $f_1(E) - f_2(E) = 1$ for $\mu_1 > E > \mu_2$, which gives:

$$I_{max} = \frac{2e}{\hbar} \frac{\Gamma_1\Gamma_2}{\Gamma} \int_{\mu_2}^{\mu_1} D_\varepsilon(E) dE, \quad (2.8)$$

where again $\mu_1 - \mu_2 = eV_b$.

For resonant tunneling, the energy level ε will be between μ_1 and μ_2 , even at low-bias. Hence, a maximum conductance will be obtained for symmetric coupling (i.e. $\Gamma_1 = \Gamma_2$):

$$G \equiv \frac{I}{V_b} = \frac{2e^2}{h} \frac{4\Gamma_1\Gamma_2}{(\Gamma_1+\Gamma_2)^2} = \frac{2e^2}{h} = G_0. \quad (2.9)$$

Having noted that the maximum conductance value for a molecular junction is the quantum of conductance, we can extend to the general case. Let us therefore define a so-called transmission function $T(E)$, related to the DOS via $D_\varepsilon(E) \frac{\Gamma_1\Gamma_2}{\Gamma_1+\Gamma_2} = \frac{1}{2\pi} \bar{T}(E)$, (at steady state conditions). With this identification, we find the so-called extended or energy-dependent Landauer formula. It describes transport in terms of transmission, summing over all possible electron energies:

$$I = \frac{2e}{h} \int_{-\infty}^{+\infty} \bar{T}(E) [f_1(E) - f_2(E)] dE. \quad (2.10)$$

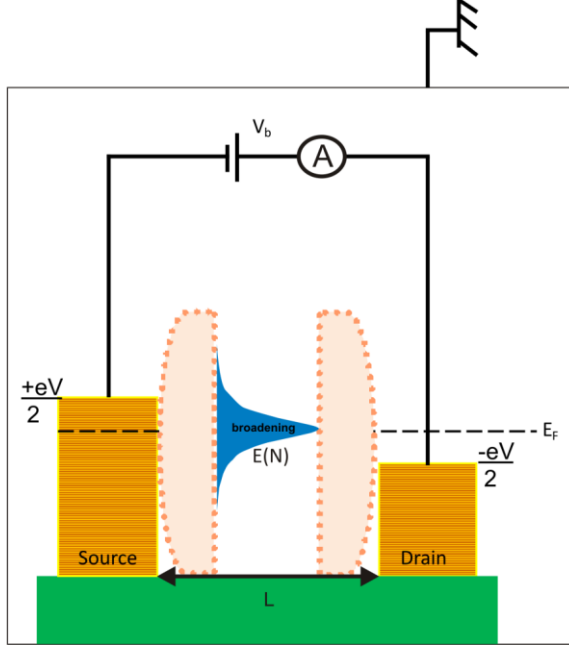


Figure 2.3: Schematic level diagram for a molecule coupled to two electrodes. In this case, the molecular level depicted is close to the electrodes' Fermi level. It broadens to a Lorentzian due to the electronic coupling to the leads. When a voltage bias V is applied, transport is described by the energy-dependent Landauer formula (see equation 2.10). In the case displayed, we have near-resonant transport.

In words, the transmission function denotes the probability [10] of electrons with a certain energy E to be transmitted through a molecular junction.

Finally, we consider the value of the potential on the molecule itself. This is determined by capacitive coupling and is given by [9]:

$$U_C = \frac{C_D}{C_E} (-eV_b), \quad (2.11)$$

assuming there is no further potential drop within the molecule. Here C_E is the total capacitance, the sum of the capacitance to the source and the drain ($C_E = C_S + C_D$). If electrostatic coupling is symmetric, the voltage drop from the left electrode to the

molecule will equal the voltage drop from the molecule to the right electrode. In that case, the electrostatic coupling parameter η has a value $\eta = 1/2$, while in general $0 \leq \eta \leq 1$. Asymmetric electrostatic coupling will generally lead to asymmetric $I(V)$ -curves, unless the transmission function is perfectly symmetric around the electrodes Fermi level. Note that electrostatic coupling should not be confused with electronic (overlap) coupling, as denoted by $\Gamma_{1,2}$. There is at best a qualitative relationship.

The transmission function can be calculated by various means, ranging from a simple tight binding approach to methods based on Density Function Theory (DFT) and non-equilibrium Green's function techniques (NEGF).

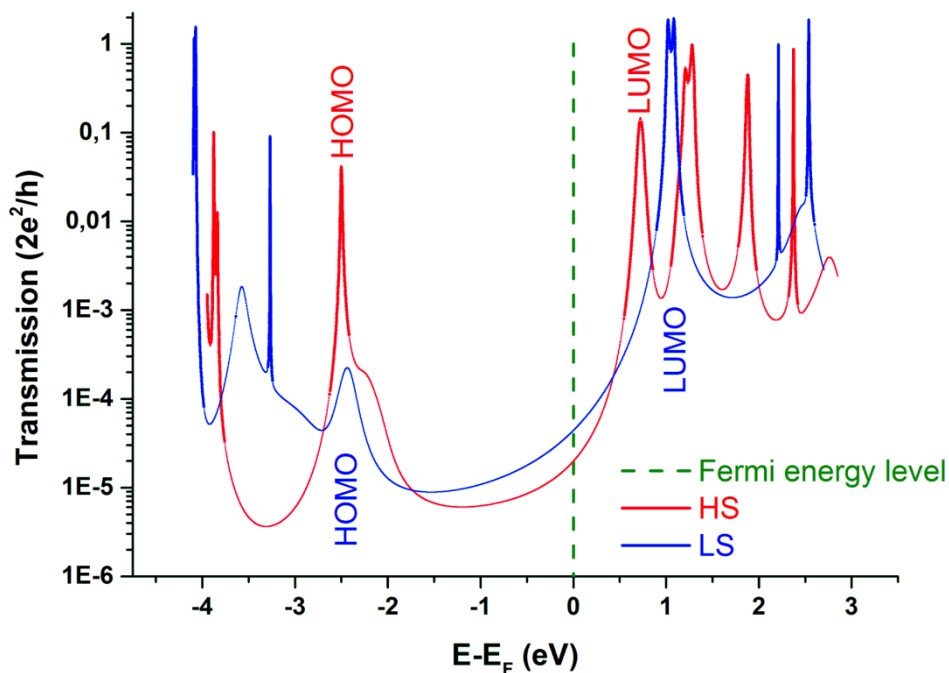


Figure 2.4: Transmission plot of a single spin crossover $\text{Fe}(\text{S-BPP})_2$ molecule coupled to gold leads [11]. The low-spin (LS) and high-spin (HS) transmission of this SCO is simulated by NEGF using B3LYP as XC-functional (calculation by Dr. V. Meded; see Chapter 6 for details).

Figure 2.4 shows the transmission function of both the low-spin and high-spin varieties of the spin crossover molecule introduced in Chapter 1 (see Figure 1.5). Note that the Fermi level of the electrodes is defined to be at 0 eV. Unfortunately, it is difficult to

independently determine the precise position of E_F for a molecular junction. The peaked nature of $T(E)$ is clearly related to the molecular energy levels. Below 0 eV, the highest occupied molecular orbital (HOMO) is marked by the first transmission peak. Above 0 eV, the first peak represents the lowest unoccupied molecular orbital (LUMO) in this nanoscale device. From the figure, it is clear that broadening varies per level. It depends on the exact electronic overlap that a particular molecular orbital has with the electrodes. Moreover, it also depends on the molecule's spin configuration. For example, the LUMO of the low-spin state is more broadened than the LUMO of the high-spin molecule. In fact, this difference in broadening is one of the reasons that theoretical predictions on how the conductance of SCO molecules should change during spin transition vary. In practice, two effects compete. On the one hand, the energy gap between the frontier orbitals (HOMO-LUMO gap) tends to decrease upon a LS to HS transition, as seen in Figure 2.4. This is intuitively expected to increase conductance, as the distance from Fermi level to the nearest level will generally decrease as well. On the other hand, the electronic coupling between the ligands at both sides of the Fe^{2+} ion decreases when going from the LS to HS state. In first approximation, the related decrease in wave function overlap should lead to a reduced transmission peak width and hence reduced conductance, as also seen in the figure. In the case of Figure 2.4, the overall effect is that the conductance is predicted to decrease for a LS to HS transition. In general, however, it is not *a priori* obvious if one should expect a conductance increase or decrease upon spin transition for a particular type of molecules. This in itself emphasizes the need for experimental data, as discussed in Chapter 6.

2.4 References

1. B. J. van Wees, H. van Houten, C. W. J. Beenakker, J. G. Williamson, L. P. Kouwenhoven, D. van der Marel and C. T. Foxon, Quantum Conductance of Point Contacts in a Two-dimensional Electron Gas, *Physical Review Letters*, **60**, (1988), 848-850.
2. D. A. Wharam, T. J. Thornton, R. Newbury, M. Pepper, H. Ahmed, J. E. F. Frost, D. G. Hasko, D. C. Peacock, D. A. Ritchie and G. A. C. Jones, One-dimensional Transport and the Quantisation of the Ballistic Resistance, *J. Phys. C: Solid State Phys.*, **21**, (1988), L209-L214.
3. Y. V. Sharvin, A Possible Method for Studying Fermi Surfaces, *Sov. Phys. -JETP*, **21**, (1965), 655-656.

-
4. J. C. Cuevas and E. Scheer, *Molecular Electronics: An Introduction to Theory and Experiment*, World Scientific, Singapore, **2010**.
 5. R. Landauer, Spatial Variation of Currents and Fields due to Localized Scatterers in Metal Conduction, *IBM J. Res. Dev.*, **1**, (1957), 223-231.
 6. M. Buttiker, Scattering Theory of Current and Intensity Noise Correlations in Conductors and Wave Guides, *Phys. Rev. B*, **46**, (1992), 12485-12507.
 7. N. Agraït, A. L. Yeyati and J. M. van Ruitenbeek, Quantum Properties of Atomic-sized Conductors, *Physics Report*, **377**, (2003), 81-279.
 8. J. M. Thijssen and H. S. J. van der Zant, Charge Transport and Single-electron Effects, *Phys. stat. sol. (b)*, **245**, (2008), 1-16.
 9. S. Datta, *Quantum Transport: Atom to transistor*, Cambridge University Press, New York, **2005**.
 10. C. Durkan, *Current at the Nanoscale: An Introduction to Nanoelectronics*, Imperial college Press, Londen, **2007**.
 11. E. J. Devid, P. N. Martinho, M. V. Kamalakar, I. Šalitroš, Ú. Prendergast, J.-F. Dayen, V. Meded, T. Lemma, R. González-Prieto, F. Evers, T. E. Keyes, M. Ruben, B. Doudin and S. J. van der Molen, Spin Transition in Arrays of Gold Nanoparticles and Spin Crossover Molecules, *ACS Nano*, **9**, (2015), 4496-4507.

